Suppression of light diffraction at the relative index of refraction close to unity. Part II

Yu.I. Terent'ev

Institute of Atmospheric Optics,
Siberian Branch of the Russian Academy of Sciences, Tomsk

Received April 20, 2007

The light diffraction on a screen is almost completely suppressed by decreasing the relative refractive index to unity in the case, when the screen is made of optically absorbing glass plates (SS8, TS2, TS3, NS12) located in different liquids.

Experimental facts of light diffraction strong weakening at values of the relative refractive index close to unity, when using the screen made of plates of absorbing glass IKS3 and SS8, which are located in a cell, filled with liquid of less optically density, are presented in Ref. 1. In connection with the partial transparency of the plates near edges, the appearance of diffraction fringes within the light beam open part can result from light diffraction at a plate and interference between directly transmitted rays and refracted rays from the partly transparent area of a plate. However, the decrease of the diffraction pattern contrast at n_{rel} decreasing to unity took place in conditions, when the plates were optically denser media, that excluded the refraction on them of the incident rays towards the beam open part. Consequently, the lines formed on the observation screen have a purely diffraction character.

Once the cell is filled with a liquid, the absorbing plates still intercept a half of the wave front. Therefore, the significant extinction of the light at $n_{rel} \to 1$ is beyond the scope of the diffraction theories based on the idea of secondary waves.

According to the rigorous Sommerfeld diffraction theory,[2] the diffraction pattern from a screen arises due to interference of the light nonintercepted by the screen with the edge light, being the light reflected from the screen edge.

If the edge light is formed only according to this theory, its intensity and, consequently, the contrast of the diffraction pattern should be different for the finite conductivity and thickness of actual screens, vanishing conductivity in dielectrics, and the use of strongly absorbing glass plates as screens. However, as a strongly absorbing IKS3 plate in air is replaced with Al or Fe plates, the relative intensity of light in diffraction patterns from them remains nearly unchanged. In Ref. 3, it was found experimentally that the light diffraction becomes significantly weaker as the thickness of the Al screen decreases down to $5.4 \cdot 10^{-2}$ μm. This fact indicates that under the Sommerfeld conditions (infinitely thin screen) the diffraction completely disappears.

The Sommerfeld theory indifference to the above factors becomes clear based on the experimental results from Ref. 4, according to which the screen edge is not the only source of the edge light. The main part of this light is formed in the area (deflection zone) above the screen, in which rays are deflected from the screen and toward the screen in roughly equally regardless of whether the screen is conductive or dielectric.

The width of this area can be judged from the experimental[5,6] dependence

$$\varepsilon = 259.5 \frac{\lambda}{0.53} / (h_s + 0.786) = \frac{489.623\lambda}{h_s + 0.786}, \qquad (1)$$

where ε are the angles of deflection of the edge rays, in min; h_s is the distance from the axis of the initial ray trajectory to the screen, in μm; 0.53 is the wavelength of the green light, in μm.

Since the light reflected from the screen is not the main source of the edge light, the significant weakening of the light diffraction at $n_{rel} \to 1$ also cannot be explained by the extinction of the reflected light at the decrease of n_{rel}.

Initially, refractive indices of the glasses used in Ref. 1 for the green light at $\lambda = 0.53$ μm were calculated as $n_c = [n_D + (n_{0.53} - n_D)]$, where n_D were borrowed from Ref. 7, and $(n_{0.53} - n_D)$ were taken equal to their values in colorless optical glasses with close n_D [Ref. 8].

It became clear in further investigations that the determined in this way n_c values somewhat differ from the measured ones, because the measured values depend on the glass melting process. As well, significant temperature dependence of the refractive indices of liquids n_{liq} was ignored.

This paper presents the results of investigation in more detail of the above effect with the use as screens of the earlier employed glasses IKS3 and SS8, as well as new glasses IKS6, TS2, TS3, and NS12. The refractive indices of this glasses and the absorption coefficients $K_\lambda = \log\tau_\lambda$ for $\lambda = 0.53$ μm (τ_λ is the attenuation of a glass of 1 mm thick), as well as their resistance to the action of the humid atmosphere and acid solutions are characterized in Table 1.

0235-6880/07/11 873-07 $02.00

Table 1. Characteristics of absorbing optical glasses

Glass brand	n_c	K_λ [Ref. 2]	Group of chemical stability	
IKS3	1.5385	> 6	C	1–3
IKS6	1.5463	> 6	B	1–3
NS12	1.5207	3.4	A	5
TS3	1.528	2.15	C	1–3
TS2	1.5279	1.06	B	1–3
SS8	1.5279	0.7105	B	1–3

Note. Group A – without risk of mildew; B – intermediate group; C – with risk of mildew; (1–3) – non-susceptible to staining; 5 – susceptible to staining.

Experiments were carried out by the scheme shown in Fig. 1 [Ref. 1], where S' is the image of the slit S (omitted); *Scr* is a thick screen lying at the distances $l = 14$ m and $L = 110$ mm, respectively, from S' and from the plane of scanning of the diffraction pattern by the slit *Sl* 50 μm wide; incident rays *1*; edge rays *2* arising due to deflection of the incident rays on the both sides from the initial direction (in the plane of the figure) in a liquid or air in the area (deflection zone) near the edge *a*; $-H$ are distances from the projection of the beam axis (PA) to fringes of the diffraction pattern formed as a result of the interference of the incident and edge rays; H are distances from PA to the points of incidence of light rays in the shadow area; K is a 12-mm wide cell with a screen installed in it at a distance of 4.4 mm from the entrance window with the plane *ab* perpendicular to the window.

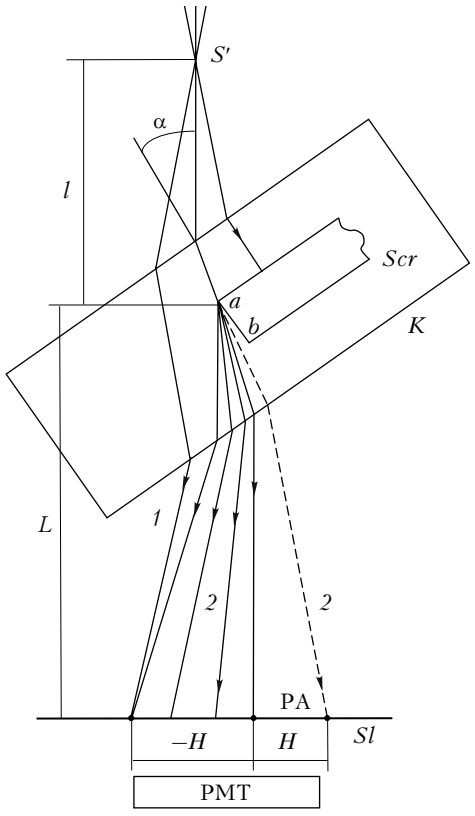

Fig. 1. Scheme of diffraction of a light beam on the screen being in air or in an optically homogeneous liquid.

The slit S is illuminated by a parallel beam of green light with $\lambda = 0.53$ μm. The widths of S and S' are equal to 23 μm. The light beam is restricted by the 5.6-mm wide slit installed in front of the objective (omitted in Fig. 1) by $\min_2$ of the diffraction pattern from S. Consequently, the fringes formed by the edge and incident rays are located within a part of central max, $\min_1$, and $\max_1$ from $S(S')$ noncovered by the screen. In the experiment, only the main part of the diffraction pattern lying in the central max was scanned. Polished plates of the glasses mentioned above and used as screens were made with the 3-mm wide plane *ab* and the right angles *a* and *b*. The cell made an angle $\alpha = 19°$ to the normal to it and the beam axis toward the direction of the plane *ab* from the beam axis in order to study diffraction patterns under classical conditions of light diffraction at the thin screen, since as the thick screen is turned about the front edge toward the direction of the plane *ab* from the incident light through angles larger than 11°, the thick screen appears to be equivalent to the thin one (razor blade).[9]

Depending on the experimental conditions, the cell was filled with dimethyl phthalate ($n_{liq} = 1.5207$ at $t_{cell} = 21.5°C$), fresh benzyl alcohol ($n_{liq} = 1.5437$ at $t_{cell} = 21.5°C$), or solutions: benzyl alcohol + + dimethyl phthalate; benzyl alcohol + naphthalene monobromide ($n_D = 1.66$); dimethyl phthalate + castor oil ($n_D = 1.4788$ at $t_{cell} = 21.25°C$).

At the given α, the plates are partly transparent near the edge *a*. Their transmittance in the case $n_{rel} = n_{cell}/n_{liq} = 1$ at different distances x from the edge is characterized in Table 2, where K_0 is the attenuation equal to the ratio of the incident light flux to the transmitted one.

Table 2. Transmittance of different glass plates at $\alpha = 19°$, $n_{rel} = 1$

Glass brand	x, μm	K_0
IKS3 IKS6	27	5.68
NS12	27.5	2.66
TS3	54.5	3.448
TS2	54.5	1.841
SS8	54	1.5206

Diffraction patterns have the highest contrast, if the edge *a* of the plates lies on the beam axis, since in this case the edge light has the highest intensity due to the maximal intensity of the axial rays.

The diffraction patterns from the IKS3, IKS6, and NS12 plates were scanned at the light flux from the slit S' attenuated by the plates to the half-maximum value. In this case, as the cell was displaced due to the partial transparency of the edge *a*, the edge passed to some distance behind the beam axis. Since these glasses are poorly transparent already at small x as compared to the beam half-width equal to 0.27 mm in the pane of the edge *a*, this passage did not lead to a significant attenuation of the intensity of edge rays.

In connection with small K_λ, the TS3, TS2, SS8 plates were introduced into the beam until the distance between max_1 and the beam axis became roughly equal to that in diffraction patterns from strongly absorbing glasses.

Table 3 summarizes the results of investigation of the diffraction patterns from the IKS3 plate in air, benzyl alcohol, or dimethyl phthalate solution in benzyl alcohol. In Table 3, I_p is the light intensity at max and min, as well as at the beam axis; I_c is the corresponding intensity without a screen in the beam; $n_{rel} < 1$ corresponds to a plate becoming less optically dense medium; $\Delta n = (n_c - n_{liq})$. According to the tabulated data, as n_{rel} decreases from n_c to 1.0005, the contrast of the diffraction patterns decreases gradually. This decrease show itself in the decreasing of the relative light intensity I_p/I_c at maxima, its increase at minima, and, consequently, attenuation of the edge light intensity.

The decrease in the contrast of fringes down to the lowest value is preceded by disappearance of fringes first at max_1 and then at min_1 from S'. This effect is easily seen due to the high contrast of the fringes caused by a smaller difference in the intensity of the rays forming these max_1, min_1, and the edge rays *2*. That is, with the decrease of n_{rel}, the flux of the edge rays, gradually attenuating, contracts to the beam axis with the simultaneous drop of the intensity in it. The facts presented are indicative of the weaker efficiency of the deflection zone at $n_{rel} \to 1$, which manifests itself in the decreased maximal angles of the ray deflection and in the smaller width of the zone. The deflection of rays should seemingly stop at $n_{rel} = 1$, and the diffraction fringes should disappear or have the minimal contrast. However, the contrast of the pattern is minimal at n_{rel} close to, but higher than 1. This fact is not a consequence of inaccurate determination of n_{rel}, since the equality of n_{rel} to unity is clearly seen from the absence of a shift in the field of view of the gradually attenuating beam, as a plate is introduced in it at $l = 0$.

As was noted in Ref. 1, this feature can be easily explained by the existence of a transition layer with $\Delta n = 0.0009$ in the IKS3 plate near the interface in the experiments considered. In this layer, the refractive index varies from its value in the depth of the plate to the refractive index of the solution during the minimal contrast of the pattern. Consequently, the relative refractive index at the interface $n_{rel.int}$ turns to be equal to unity.

According to Ref. 1, the incomplete disappearance of light diffraction at $n_{rel.int} = 1$ is likely caused by the action of atoms of the screen substance lying not only at the interface, but also in some depth, where $n_{rel} \neq 1$ due to existence of the transition layer, on the deflected rays. According to this, the screens of glasses with smallest Δn in the transition layer should cause the maximal weakening of the diffraction at $n_{rel.int} = 1$.

Due to the smallest number of the deflected rays *2*, when $n_{rel.int} = 1$, and to the deflection of the rays passing through the area of the plate edge *a* to small angles at $n_{rel} \leq 1.0005$, the light intensity at the beam axis achieves the highest value.

As n_{rel} decreased down to 1, $n_{rel.int}$ became smaller than 1. This resulted in the increase of the intensity of edge rays *2* due to intensification of the deflection zone and the appearance of refracted rays propagating toward the diffraction pattern from the transition layer (which became a less optically dense medium compared to the solution). The contrast of diffraction fringes increased as a result of the joint interference of rays *2* and the refracted rays with rays *1*.

At $n_{rel} = 0.9992$, all the plate becomes a less optically dense medium. Therefore, near the edge *a* it refracts rays toward the diffraction pattern at an area having a larger width as compared to the width of the transition layer, and, consequently, the rays have a higher intensity. Simultaneously, the intensity of rays *2* increases due to the increase of $(n_{liq} - n_{int})$, where n_{int} is the refractive index of the plate at the interface between media. The increase in these

Table 3. Relative light intensity in diffraction patterns from the IKS3 plate at different values of the relative refractive index (α = 19°)

Fringe	Plate						
	Denser medium; in solution; $n_{rel} = 1.0042$ $\Delta n = 0.0053$ $t_{cell} = 21.3$°C	in air	Denser medium; in solution; $n_{rel} = 1.0007$ $\Delta n = 0.0011$ $t_{cell} = 21.5$°C	Denser medium; in solution; $n_{rel} = 1.0005$ $\Delta n = 0.0009$ $t_{cell} = 21.6$°C	in solution; $n_{rel} = 1$; $t_{cell} = 21.5$°C	Less dense medium; in solution; $n_{rel} = 0.9992$; $\Delta n = -0.0012$ $t_{cell} = 22$°C	Less dense medium; in benzyl alcohol; $n_{rel} = 0.997$ $\Delta n = -0.0046$ $t_{cell} = 22$°C
	I_p/I_c						
max_1	1.313	1.37	1.247	1.193	1.3213	1.577	1.389
min_1	0.796	0.742	0.867	0.881	0.822	0.609	0.648
max_2	1.224	1.324	1.134	1.077	1.168	1.5236	1.287
min_2	0.83	0.783	0.916	0.932	0.8695	0.6846	0.611
max_3	1.211	1.218	1.1	1.026	1.101	1.53	1.276
min_3	0.813	0.773	0.939	0.918	0.8793	0.703	0.61
max_4	1.138	1.311	1.039	1.00	1.0483	1.475	1.382
min_4	0.815	0.718	0.833	0.917	0.9534	0.741	0.554
max_5	1.434	1.215	–	–	–	1.4444	1.636
PA	0.258	0.235	0.274	0.4183	0.2535	0.272	0.505

intensities results in the sharp increase of the contrast of diffraction fringes at the open part of the central maximum from S'. At the same time, fringes at $\min_1$ and $\max_1$ from S' remain weak. With the following decrease of n_{rel} down to 0.997, the refracted rays shift from the main part of the pattern to $\min_1$ and $\max_1$ from S' due to the increase of the refraction angles. As a result, the contrast of the pattern decreases again, but remaines significant due to the continuing intensification of the deflection zone with the increase of $(n_{liq} - n_{int})$, while the contrast and brightness of the fringes at $\min_1$ and $\max_1$ from S' increase sharply.

Table 4 summarizes the information on weakening of the diffraction pattern from the IKS6 plate at $n_{rel} \to 1$, demonstrating that the minimal contrast of the pattern in this case is roughly identical to that from the IKS3 plate and establishes at $n_{rel} > 1$ as well. Consequently, there is a transition layer in the IKS6 plate too.

Table 4. Relative light intensity in diffraction patterns from the IKS6 plate at different values of the relative refractive index (α = 19°)

Fringe	Plate		
	in solution; n_{rel} = 1.0022 Δn = 0.0035 t_{cell} = 21 °C	in benzyl alcohol; n_{rel} = 1.0012 Δn = 0.002 t_{cell} = 21 °C	in solution; n_{rel} = 1 t_{cell} = 21 °C
	I_p/I_c		
$\max_1$	1.298	1.217	1.35
$\min_1$	0.8074	09447	0.822
$\max_2$	1.1804	1.079	1.189
$\min_2$	0.8641	0.96	0.883
$\max_3$	1.202	1.0454	1.1355
$\min_3$	0.8974	0.9766	0.9627
$\max_4$	1.1875	1	1.1
$\min_4$	0.8636	1	0.9583
$\max_5$	1.3	1.056	1.2
PA	0.337	0.3805	0.284

The degree of fringe weakening at the minimal contrast of the pattern is illustrated in Fig. 2, where I is the light intensity in relative units in the scanning plane; curves *1* and *2* characterize the intensity distribution, respectively, with and without screen in the beam.

When the SS8, TS2, and TS3 plates serve as screens, the diffraction patterns have the lowest contrast at $n_{rel} = 1$ (Table 5). Consequently, there is no transition layers in these plates. Under the conditions considered, periphery fringes are completely absent, while the others, except for $\max_1$, are vanishing.

It is seem that as n_{rel} deviates from 1, the contrast of the pattern increases again, and this increase is especially drastic at a small decrease of n_{rel}, leading to refraction of rays from the plates toward the diffraction pattern and to their incidence on the pattern.

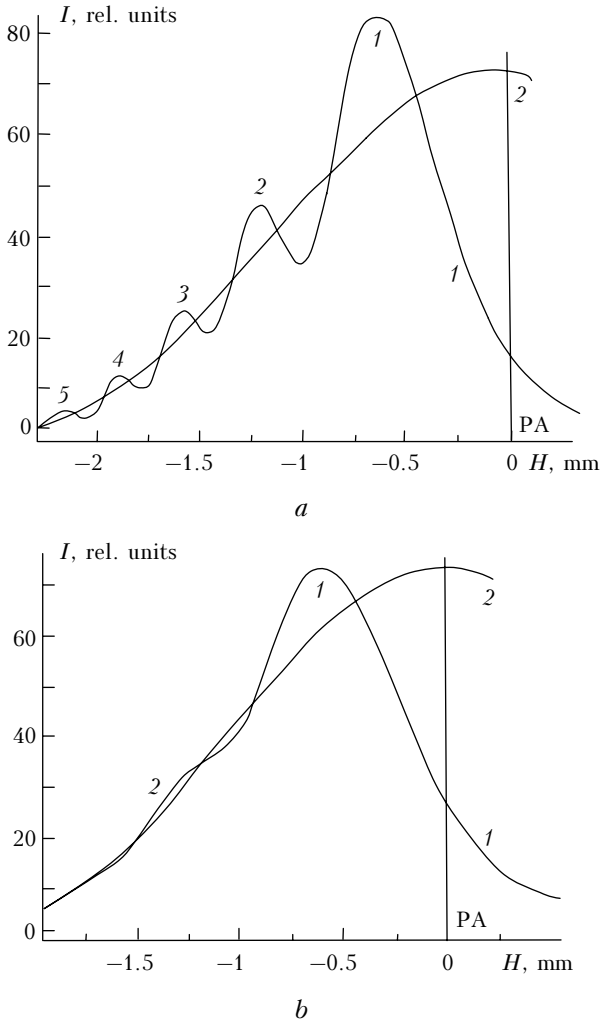

Fig. 2. Diffraction patterns from the IKS6 plate: in air (*a*) and in benzyl alcohol at n_{rel} = 1.0012 (*b*).

The abnormally high increase in the contrast of fringes in the pattern from TS3 at $\Delta n = -0.004$ is likely caused by the incidence of the most intense part of refracted rays within the pattern and by the absence of path length difference between them and rays *2,* or a small path length difference as compared to $\lambda/2$.

According to Table 6, the diffraction pattern from the strongly absorbing NS12 plate, similarly to the patterns from the SS8, TS2, and TS3 plates, has the lowest contrast at $n_{rel} = 1$. This fact indicates the absence of the transition layer in the plate. At the same time, the contrast itself is as low as that in the pattern from SS8.

The character of the light intensity distribution in the considered pattern (Fig. 3) demonstrates that light diffraction nearly terminates at the absorbing plates having no transition layer at n_{rel} = 1.

Among the glasses listed above, the NS12 glass is most suitable for practice, since it is strongly absorbing, and the equality of n_{rel} to unity is provided by placing the glass in the homogeneous liquid.

Table 5. Relative light intensity in diffraction patterns from the SS8, TS2, and TS3 plates at different values of the relative refractive index (α = 19°)

Fringe	SS8			TS2	TS3		
	Denser medium; in dimethyl phthalate; $n_{rel} = 1.0049$ $\Delta n = 0.0076$ $t_{cell} = 21°C$	in solution; $n_{rel} = 1$; $t_{cell} = 21.8°C$	Less dense medium; in solution; $n_{rel} = 0.9998$ $\Delta n = -0.0002$ $t_{cell} = 21.3°C$	in solution; $n_{rel} = 1$; $t_{cell} = 21.2°C$	Denser medium; $n_{rel} = 1.0004$ $\Delta n = 0.0007$ $t_{cell} = 21.4°C$	$n_{rel} = 1$; $t_{cell} = 21.2°C$	Less dense medium; $n_{rel} = 0.9973$ $\Delta n = -0.004$ $t_{cell} = 21.4°C$
	I_p/I_c						
max_1	1.2974	1.0826	1.6283	1.143	1.2196	1.1494	2.3154
min_1	0.8	0.9976	0.8024	0.95	0.8648	0.94	0.281
max_2	1.191	1.021	1.195	1.063	1.1224	1.025	3.604
min_2	0.844	0.993	0.888	0.979	0.8376	0.965	0.333
max_3	1.171	1.0245	1.17	1.033	1.1956	1	3.167
min_3	0.85	0.9954	0.937	0.92	0.875	1	0.45
max_4	1.17	1	1.063	1	1.05	1	2.526
min_4	0.845	0.9906	1	1	–	1	0.538
max_5	–	1	1	1	–	1	3.04
PA	0.315	0.74	0.419	0.671	0.303	0.4194	0.1226

When S' is installed at the position corresponding to $l = -14$ mm, the diffraction pattern displaces from the left (now intercepted) half of central max_1 from S' to the right one due to interference of rays *1* with rays *2* deflected toward the screen shadow rather than from the screen. In this case, the contrast of the patterns from the plates having no transition layer at $n_{rel} = 1$ is as low as at $l = 14$ mm. Consequently, under the conditions considered the intensity of rays *2,* deflected in the deflection zone, decreases to the same extent regardless of the direction of their deflection. Therefore, the light incident onto the screen shadow in the absence of the transition layer and at $n_{rel} = 1$, is the main light passing without refraction through the partly transparent area of the edge *a* of the plate. Propagating within the initial boundaries of the beam, it does not lead to the increase of the angular width of the beam.

Table 6. Relative light intensity in the diffraction pattern from the NS12 plate at different values of the relative refractive index (α = 19°)

Fringe	Plate		
	Denser medium; in solution; $n_{rel} = 1.0013$ $\Delta n = 0.002$ $t_{cell} = 21.1°C$	in dimethyl phthalate; $n_{rel} = 1$; $t_{cell} = 21.7°C$	Less dense medium; in solution; $n_{rel} = 0.9994$ $\Delta n = -0.0008$ $t_{cell} = 21.6°C$
	I_p/I_c		
max_1	1.2572	1.0718	1.677
min_1	0.8526	0.9966	0.806
max_2	1.144	1.0394	1.25
min_2	0.8834	0.931	0.892
max_3	1.119	1.0538	1.157
min_3	0.8363	0.93	0.914
max_4	1.1875	1.0744	1.0476
min_4	0.913	0.9542	0.806
max_5	1.25	1	1
min_5	–	1	0.86
PA	0.293	0.416	0.098

According to Ref. 4, the deflection zone, similarly to the electric field, is most intense near the screen edges. Based on the above dependence of the efficiency of ray deflection in the zone on the relative refractive index, this fact is likely indicative of the higher value of the refractive index near edges as compared to that at some distance from them. Consequently, $n_{rel} = 1$ near the edge *a* of the plate somewhat decreases at a distance from the edge, thus causing the deflection zone intensification.

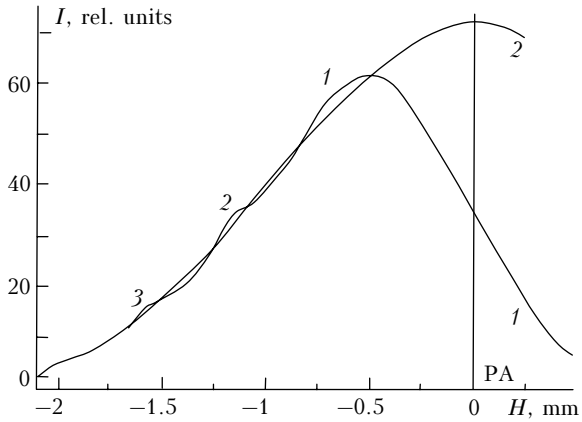

Fig. 3. Diffraction pattern from the NS12 plate in dimethyl phthalate, $n_{rel} = 1$.

In the case of gradual decrease of α at $n_{rel} = 1$, the path length of rays deflected in the zone increases near the edge *a*, and the increasing part of the path lies far from the edge, that is, in the intensified zone. As a result, the deflection angles and the intensity of the deflected rays increase, leading to a higher contrast of the diffraction pattern (Table 7).

The diffraction pattern, vanishing at $\alpha = 19°$, becomes highly contrast at $\alpha = 0$, since in this case the edge rays are deflected at the whole length of the zone or until they leave the zone due to the deflection.

Due to the strong temperature dependence of the refractive index of liquids (as the temperature decreases by 1°, n_D of dimethyl phthalate increases roughly by 0.0005), the contrast of the diffraction pattern at $n_{rel} = 1$ is sensitive to temperature drop, which transforms the liquid into an optically denser medium. As a consequence, some refracted rays fall from the vicinity of the edge a of the plate onto the pattern, thus increasing its contrast. Therefore, the poorly contrast pattern from NS12 (see Table 7: $\alpha = 5°$; $t_{cell} = 22.1°C$) became contrast, as t_{cell} decreased down to 20.9°C.

Table 7. Character of variation of the relative light intensity in the diffraction pattern from the NS12 plate at variation of α and temperature

Fringe	$n_{rel} = 1$; $\alpha = 5°$; $t_{cell} = 22.1°C$	$\alpha = 5°$; $t_{cell} = 20.9°C$	$n_{rel} = 1$; $\alpha = 0$; $t_{cell} = 22.1°C$
	I_p/I_c		
max_1	1.16	1.4545	1.6555
min_1	0.919	0.6871	0.603
max_2	1.033	1.2836	1.4916
min_2	0.957	0.798	0.6986
max_3	1.1014	1.227	1.5097
min_3	0.851	0.772	0.655
max_4	1.111	1.212	1.893
min_4	–	0.761	0.6944
max_5	–	1.111	1.727
PA	0.345	0.262	0.17

As α decreases from its initial value to 0 at $n_{rel} = 1$, the diffraction pattern from the SS8 plate having the minimal contrast becomes highly contrast similarly to the pattern from the NS12 plate (Table 8, first column). The following decrease of the refractive index of the liquid by only 0.00016 results in disappearance of fringes at max_1 and min_1 from S' and in attenuation of the main part of the pattern down to the level characterized by the second column.

Table 8. Character of variation of the relative light intensity in the diffraction pattern from the SS8 plate at decrease of its contrast to the minimal value caused by increase of n_{rel} from 1 to 1.0001

Fringe	$\alpha = 0$, $t_{cell} = 21°C$	
	$n_{rel} = 1$	$n_{rel} = 1{,}0001$
	I_p/I_c	
max_1	1.615	1.55
min_1	0.58	0.668
max_2	1.55	1.434
min_2	0.605	0.655
max_3	1.52	1.443
min_3	0.592	0.718
max_4	1.508	1.37
min_4	0.609	0.639
PA	0.209	0.181

In the case of repeated decrease of n_{liq} by roughly the same value, contrast fringes again appear at max_1 and min_1 from S' and the contrast of the main pattern increases.

This change in the contrast confirms the small increase of n_c near screen edges. Thus, after the first decrease of n_{liq}, n_{rel} becomes equal to 1 at a distance from the edge a and higher than 1 near the edge. This results in intensification of the zone near the edge and its nearly complete disappearance far from the edge. Since $\alpha = 0$, deflected rays mainly pass through the part of the zone lying far from the edge a. Weakening of the zone at the edge causes the decrease in deflection angles and intensity of edge rays. After the second decrease of n_{liq}, n_{rel} near the edge, a decreases even greater, and far from the edge n_{rel} becomes higher that 1. As a result, the zone intensifies all over its length, and this results in stronger diffraction of the light.

The IKS6, SS8, TS2, IKS3, and TS3 glasses fall in the same group of chemical resistance. However, the transition layer is formed only in the infrared glasses. This is likely caused by the release of some component, possibly, selenium [10] from the surface layers of the glasses.

The deflection of light rays in the deflection zone lying above the screen and its features can be easily explained based on the Newton hypothesis about the existence of the remote interaction between light particles and bodies,[11] if a light ray is understood as a trajectory of motion of a light particle (photon).

In this case, the character of the diffraction pattern should depend on the amount of the screen substance within the range of the marked action of the force deflecting a photon. This dependence actually exists. This follows from the experimental data,[3] indicating the significant decrease in the relative intensity of diffraction fringes with the decrease of the thickness and density of the screen substance down to small values.

It is well-known that the photon energy is $m_{ph}c^2 = h_P\nu = h_Pc/\lambda$, where m_{ph} is the photon mass, in g; c is the speed of light, in cm/s; h_P is the Planck's constant; ν is the frequency of light; λ is the wavelength, in cm. Hence, λ, in μm, $= 10^4 h_P/m_{ph}c$ and

$$\varepsilon = \frac{489.623 \cdot 10^4 h_P}{m_{ph}c(h_s + 0.786)}. \quad (2)$$

If we accept the reality of the force acting on the photon from the screen, then ε, rad $= \tan\varepsilon = v/c$, where v is the velocity imparted by the force F to the photon in the direction perpendicular to its initial direction for the time t. Since $v = Ft/m_{ph}$, ε, rad $= Ft/m_{ph}c =$ ε, min/57.3° · 60′ = ε, min/3438′;

$$\varepsilon, \text{ min} = 3438' Ft/m_{ph}c. \quad (3)$$

Equating Eqs. (2) and (3), we obtain after some transformation

$$Ft = 1.424 h_P/(h_s + 0.786). \quad (4)$$

This equation shows that the impulse of the force acting on the photon is independent of the photon mass and the frequency of the light $\nu = m_{ph}c^2/h_P$ (frequency of the elementary light wave associated with the photon[12]) and at $h_s \gg 0.786$ it decreases in the inverse proportion to h_s.

The value of t is determined by c and the path length of photons in the deflection zone, which is the same for photons of different mass in the case of identical h_s. Therefore, the force acting on the photon is also independent of the photon mass and, consequently, of the frequency of light ν.

The dependence of light diffraction on the relative refractive index and its almost complete disappearance at $n_{rel} = 1$ should be of undoubted interest for in-depth understanding of the essence of interaction of light with matter and in practical purposes.

The Huygens—Fresnel principle, which easily explains the absence of light diffraction on a transparent screen at $n_{rel} = 1$, contradicts the experimental results presented. This indicates the absence of secondary waves in reality.

References

1. Yu.I. Terent'ev, Atmos. Oceanic Opt. **20**, No. 1, 9–11 (2007).
2. M. Born and E. Wolf, *Principles of Optics* (Pergamon, New York, 1959).
3. Yu.I. Terent'ev, Atmos. Oceanic Opt. **16**, No. 4, 283–287 (2003).
4. Yu.I. Terent'ev, Atmos. Oceanic Opt. **8**, No. 4, 262–268 (1995).
5. Yu.I. Terent'ev, Atmos. Oceanic Opt. **11**, No. 12, 1088–1092 (1998).
6. Yu.I. Terent'ev, Atmos. Oceanic Opt. **17**, No. 7, 482–484 (2004).
7. *Catalog of Colored Glass 117* (Mashinostroenie, Moscow, 1967), 61 pp.
8. *Colorless Optical Glass*. USSR State Standard No. 3514-76 (Standards Press, Moscow, 1968), 74 pp.
9. Yu.I. Terent'ev, Atm. Opt. **4**, No. 5, 347–350 (1991).
10. M.N. Semibratov, *Technology of Optical Parts* (Mashinostroenie, Moscow, 1978), 416 pp.
11. U.I. Frankfurt, *Creators of Physical Optics* (Nauka, Moscow, 1973), 351 pp.
12. G.S. Landsberg, *Optics* (GIT-TL, Moscow, 1957), 759 pp.